AIAA 79-0949R

Satellites for the Detection of Nonsolar Planets

Lothar W. Bandermann* and Richard H. Pohle†
Lockheed Palo Alto Research Laboratories, Palo Alto, Calif.
and
James P. Murphy,‡ John W. Vorreiter,§ and David C. Black¶
NASA Ames Research Center, Moffett Field, Calif.

Two sensor systems for the direct detection of nonsolar planets from Earth orbit are evaluated: 1) an apodized visual telescope (APOTS), and 2) a spinning infrared interferometer (IRIS). Their performance characteristics and technology requirements for a five-year mission are determined. The simpler instrument, APOTS, requires a substantial improvement in mirror fabrication techniques before it can approach its full performance potential. The IRIS requires technology development in the areas of long-lifetime cryogenic systems and of active control techniques. Technology issues of secondary importance are discussed.

I. Introduction

THERE are two methods of nonsolar planet detection: 1) *indirect* observation, i.e., observing the parent star and inferring the presence of a planet from its perturbing influence on the motion of the star relative to us; and 2) *direct* observation of the planet.

Indirect methods require the intercomparisons of several stellar position or radial velocity measurements taken years apart. Observations made from the ground of the positions of some nearby stars (e.g., Barnard's star) in the past have yielded inconclusive results, partly because of the difficulties of comparing different photographic plates, finding proper stellar reference frames, and accounting for the motions in the Earth's atmosphere and of the Earth itself. However, recent advances of instrumentation and theoretical analysis suggest that ground-based indirect methods may eventually be effective in a nonsolar planet search of nearby stars.

With direct methods, one faces the problem of resolving an extremely weak point source (planet) from a nearby bright source (parent star) against a strong background (zodiacal light). Instruments of ultrahigh sensitivity, spatial resolution, and background discrimination are required. They must have large apertures and be above the Earth's atmosphere.

We have studied the performance characteristics and the technology requirements of two sensor systems proposed for the direct detection of nonsolar planets from an Earth orbit; and apodized visual telescope (APOTS) and a spinning infrared interferometer (IRIS). The mission objectives for which these systems would be designed are to detect any large planets, if they exist, around nearby bright stars; to accumulate statistics of such planets; and to determine basic planet properties such as the orbit radius. Important study constraints were to assume for each sensor system: 1) one Shuttle (STS) deployment using full STS capacity but requiring no on-orbit assembly; 2) a 5-yr operational life without reservicing; and 3) optimized sensor performance for a standard extrasolar planet. This paper discusses important results of the study.

To compare the performances of the two sensors sytems, we assume the same primary mirror diameter for each, namely, 3 m. This value is near the limit of both current manufacturing capabilities for high-quality mirrors and the STS payload bay limitations. Much larger mirrors would have to be segmented. Problems of deployment and segment phasing could compromise the feasibility of the sensor systems.

II. Performance Criteria

In the complete absence of information about other planetary systems, our solar system serves as the example for which we shall define a nominal task of planet detection. That task primarily serves to derive and compare nominal performance and technology requirements for the two sensors. Although reasonable, our model planet system is nevertheless somewhat arbitrary. However, some important conclusions about detecting other types of systems can easily be drawn from this study. To simplify the analysis, we confine the nominal task to detecting the brightest of the planets, and we ignore the possible influence of the presence of sister planets on the sensor performance. (Surely this point must be carefully reconsidered in subsequent studies.) Thus, the nominal planet-star is Jupiter-sun, as seen from a distance of 10 parsecs (32 light-years). The situation is illustrated in Fig. 1. The standard planet-star separation is 2.0 μrad (0.41 $\S$,) which is the value for a random orientation of the planet orbit relative to us.

Within that distance there are at least a dozen single stars brighter than the sun at 10 parsecs (5th magnitude). Since it is

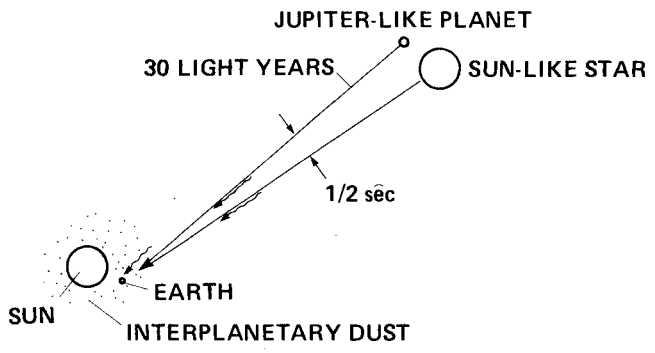

Fig. 1 Standard star-planet system.

Presented as Paper 79-0949 at the AIAA/NASA Conference on Advanced Technology for Future Space Systems, Hampton, Va., May 8-11, 1979; submitted Feb. 7, 1980; revision received July 10, 1980. This paper is declared a work of the U.S. Government and therefore is in the public domain.

*Research Scientist, Electro-Optics Laboratory.
†Staff Scientist, Electro-Optics Laboratory.
‡Assistant Chief, Project Technology Branch.
§Research Scientist, Project Technology Branch. Member AIAA.
¶Research Scientist, Theoretical and Planetary Studies Branch.

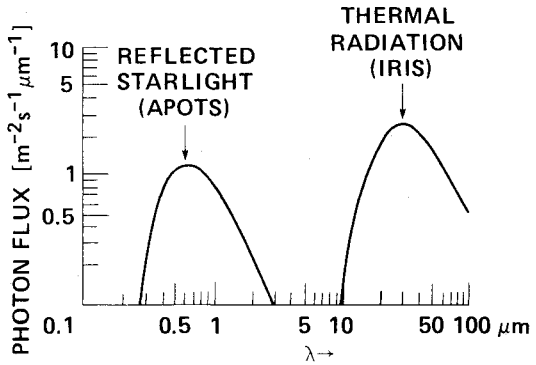

Fig. 2 Radiation from standard planet.

Table 1 Planet detection: visible vs infrared

	Visible (0.6 μm)	Infrared (26 μm)
Photon flux from standard planet, $m^{-2}s^{-1}\mu m^{-1}$	1.4[a]	2.5
Radius of Airy disk,[b] μrad	0.24	12
Photon rate on Airy disk of planet, $s^{-1}\mu m^{-1}$:		
By star	1.3×10^6	1.2×10^6
By planet	7	15
By zodiacal light[c]	3	3000

[a] Averaged over planet's phases. [b] Telescope aperture 3 m. [c] Ecliptic poles.

reasonable to presume that, if any at all, many of the fainter stars as well as the brightest ones would have planets, there would be a reasonable number of candidate stars for a 5-yr search.

The standard planet has solar spectral distribution in the visible and is a blackbody at 125 K in the infrared (Fig. 2). Hence, the planetary photon flux has maxima at 0.6 and 30 μm, which are candidate wavelengths of operation for the APOTS and IRIS, respectively. In both cases, the photon flux from the planet in the focal plane is overwhelmed by background light from the parent star by a factor of $\sim10^5$ (see Table 1).

Although both sensors must overcome a similar star-planet photon ratio, the methods of separating the planet from the star must be different. That is because in the visible (APOTS) the planet image is well outside the star's Airy disk, while in the infrared (IRIS) it is buried well inside. Therefore, the APOTS uses apodization, and the IRIS uses interferometry to separate the diffraction images.

We take planet detection to mean determining the presence of a faint point-like object near a star under observation with an angular separation from the star and a brightness appropriate for a planet. Clearly, following detection, additional evidence must be obtained to conclusively show that the faint object is indeed a planet rather than a background object of another kind. The necessary evidence can be obtained by measuring the object's temperature (of which the IRIS is capable but not the APOTS) or determining its orbit around the candidate star. Orbit determination can be accomplished with either sensor system during the assumed 5-yr lifetime of the experiment (Jupiter's orbital period is 11.8 yr). The choice and sequence of candidate stars will be influenced by the time interval between observations as well as by the observability of the stars from the chosen Earth orbit.

An important measure of sensor system performance is the observation time required for the detection of the standard planet, i.e., the detection time, for a given level of confidence. Detection occurs when a set threshold signal-to-noise (S/N) is exceeded by any sensor channel. The threshold is based on a false alarm rate of 10% and a missed detection rate of 1%. The relatively large false alarm rate is allowed since the sensor will look again. However, the number of missed detections must be small since a few missed detections in a limited sample will skew the calculated planet statistics.

Table 2 Apodized telescope (APOTS)

Overall dimensions: Shuttle cargo bay limits (4 m × 18 m)
Total mass: 6900 kg
Structure: Aluminum except for graphite/metal metering truss
Orbit: 550-km circular, 28.5-deg inclination
Delivery and deployment: Shuttle plus orbit boost engine, no on-orbit assembly
Operational life: 5 yr, no reservicing
Optics:
Primary mirror: 3-m diam, f/5, off-axis, parabolic, figure controlled
Secondary: 10-30-cm diam
Configuration: Focal, Gregorian
Wavelength of operation: Visible spectrum (0.4-0.8 μm)
Detectors(s): Cooled CCD (charge-coupled device) mosaic

III. Apodized Telescope: Description and Performance

In the visible, the observation time for detecting the standard planet can be reduced by suppressing the diffraction rings of the parent star. Apodization, the gradual reduction of the pupil transmission from unity at the aperture center to zero at the edge, is a well-known technique to reduce the ratio of the brightness in the rings to that in the central disk. Although wasteful of photons, apodization increases the S/N ratio of the planet image. We refer to B. Oliver for the details of this technique.[1]

The APOTS is a conventional two-mirror telescope in off-axis Gregorian configuration with a transmitting apodizing mask at the primary mirror image. A schematic layout is shown in Fig. 3, and the key systems parameters are given in Table 2. The primary mirror is parabolic, with the prime focus located within the Shuttle bay, about 15 m from this mirror; the focal ratio of the parent optics is f/2.5.

The primary mirror is adaptively figured in real time by a figure sensor-actuator control loop. The telescope is enclosed in a 17-m long baffle tube to reduce primary mirror illumination from out-of-field sources.

Scattered light in the APOTS focal plane is further reduced by superpolishing all mirror surfaces to 10-Å microroughness and by enclosing the secondary mirror and the apodizing mask in a tube pierced only by a pinhole (field stop). The system focal ratio is chosen to match the size of the apodized planet image to a detector resolution element in such a way as to maximize the S/N ratio. Apodization enlarges the planet image, i.e., the central diffraction disk, and the field-of-view (FOV) of single detector element, a pixel of a cooled charge-coupled device (CCD) mosaic, must be ~0.4 μrad.

To calculate the detection time for the APOTS, we assume an apodizer plate with a Sonine transmission, i.e., the transmission as a function of distance r from the plate center is equal to $(1-r^2/R^2)^\mu$, where R is the aperture image radius and $\mu\geq0$; μ corresponds to a clear (unapodized) aperture. For $\mu=6$ (APOTS 6), the ratio of star-to-planet Airy disk brightness (at the planet's image location) is only ~1 compared with 10^5 for the clear aperture. As a consequence, there has been a substantial gain in S/N but at a loss of 85% of planet photons. These results assume a perfect mirror; the point will be discussed later. For minimum zodiacal light and reasonable values for detector efficiency, optical transmission (apart from apodizer transmission), and no stray light, we find a detection time of 0.9 h for the APOTS 6 as compared with $\sim10^3$ h for the clear aperture, APOTS 0.

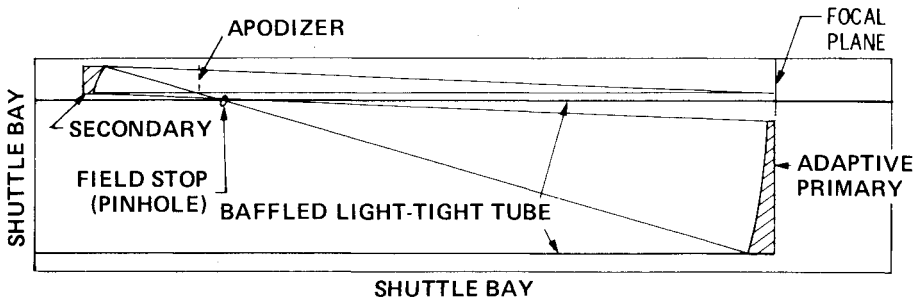

Fig. 3 Apodized telescope.

Figure 4 shows how the detection time t varies with key planet parameters: orbit radius δ, sensor-planet distance d, and angular separation from the star θ. Notice 1) the very rapid increase of t with increasing values of d and decreasing values of θ; 2) the minimum of t as a function of δ, which results from the competition between change of brightness of the planet and angular separation from the star; and finally, 3) for $\theta \gg 2$ μrad, $t \sim$ constant because at large angular separations stellar diffraction (as apodized) is small compared with the zodiacal light.

It will be discussed in the following section that the requirements for the APOTS mirror figure control necessary to achieve the preceding performance are extraordinarily stringent and represent the key technology issue for the APOTS. For this reason, a very high apodization $\mu > 6$ is unreasonable because its advantages cannot be realized. Indeed, an apodization level corresponding to $\mu \leq 2$ can now be realized. For that case (APOTS 2), the detection time is ~100 h, still better by a factor 10 than for a clear mirror. The depndences of extra-solar planet observation time on d, δ, and θ for the APOTS 2 are shown in Fig. 4b. The zodiacal light background is always negligible compared with diffracted star light.

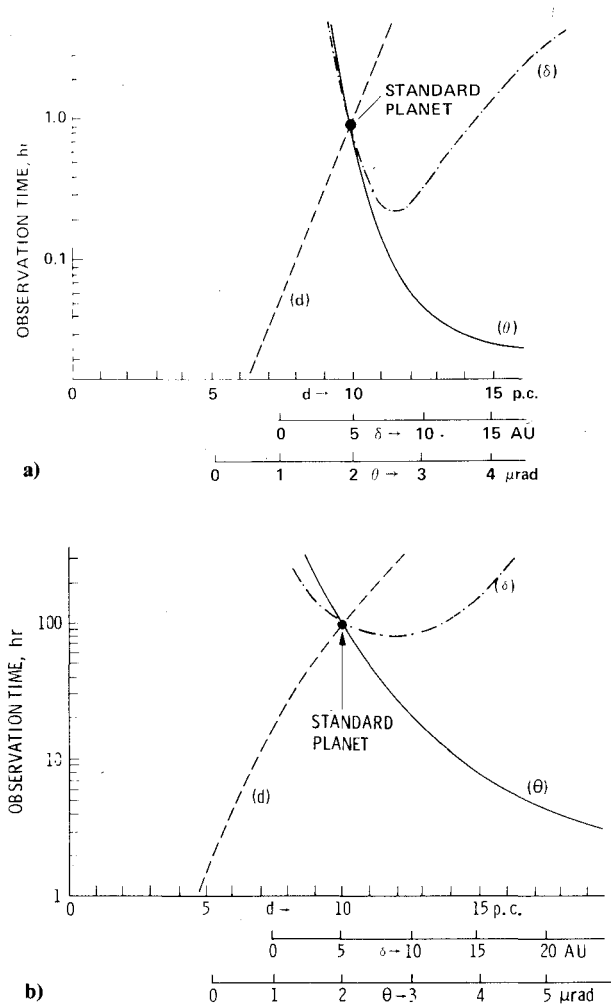

Fig. 4 APOTS performance with Sonine Rh mask: a) $\mu = 6$, b) $\mu = 2$.

IV. APOTS: Technology Issues

Mirror Ripple

Mirror and telescope figure errors can be categorized as aberrations, figure ripple, or surface roughness. The APOTS is very sensitive to ripple: undulations in the mirror figure of 5-50 cycles across the aperture. Ripple on the primary and secondary mirrors and the apodizer mask add pointwise and have a grating effect on the wavefront. As a result, light is diffracted from the central disk to the rings (where the planet image lies). Ripple thus removes the virtue of apodization which is stellar image ring suppression. Therefore, sensing and control of wavefront ripple are issues greatly affecting the APOTS feasibility.

Mirror ripple severely affects the detection time, as shown by Fig. 5. To realize the potential of apodization for extra-solar planet detection (e.g., for $\mu = 6$), ripple must be held below atomic dimensions. We know of no proven technique to accomplish this kind of control. Easing the mirror ripple requirements to 30 Å, a goal and not yet an achievement for the Space Telescope, lowers the useful apodization to $\mu = 2$ and therefore results in a degraded APOTS performance.

The long APOTS 2 detection times will require frequent target reacquisitions (caused by observation interruptions due to stray light requirements), increased demand for on-board data processing, and increased vulnerability to sensor drifts.

Even if ripple-free mirrors could be manufactured, total telescope figure must be maintained in an orbital environment continuously throughout an observation period. Therefore, active control of the figure is required.

Since three to four actuators per cycle of ripple are required, a large number of actuator control channels would be needed. The actuators would be concentrated near the primary mirror center where the presence of ripple has the greatest harmful effect. The required actuator range need not be large for a well figured and stable mirror; therefore, electrostriction (produced by voltages applied across the mirror face plate between the front surface coating and rear electrodes) might be an effective technique for ripple control actuation.

Proper actuation requires accurate wavefront sensing. If the wavefront from the parent star is used, the complete image ring structure is required; a sampling of the unusable central rings of the star image would not suffice. A beam splitter placed after the apodizer mask could divert a portion of the stellar wavefront into a wavefront sensor at the expense of additional ripple and scattered light. As an alternative, one could consider putting a phase or amplitude grating on the apodizing mask itself to diffract light into the wavefront sensor. An acromatizing grating would probably be required.

In summary, mirror ripple control is the paramount feasibility issue and technology driver for the APOTS.

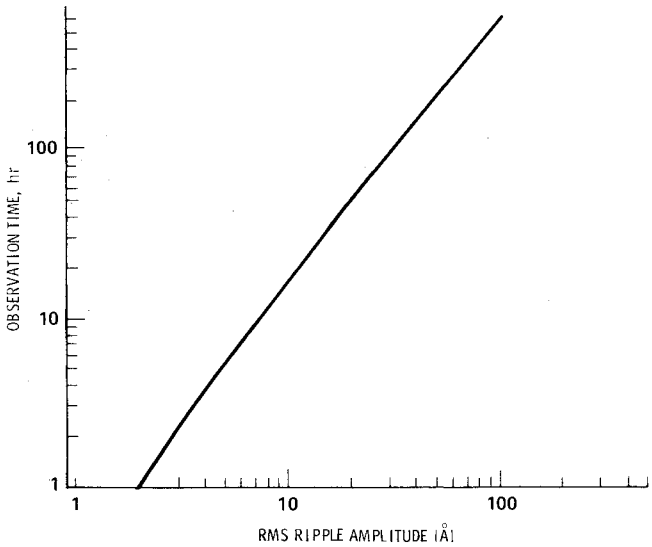

Fig. 5 Effect of scattered light on APOTS integration time.

Table 3 APOTS optical alignment tolerances (in μm) for a 3-m-diam mirror

	Unapodized ($\mu = 0$)	APOTS 2 ($\mu = 2$)	APOTS 6 ($\mu = 6$)
Axial	19	23	34
Lateral	930	1130	1670
	(Strehl ratio = 0.9)		

Pointing and Alignment

Misalignment of the telescope has three deleterious effects: 1) a displacement of the source image in the focal plane, 2) a reduction of the intensity of the central disk of the image, and 3) an increase in the amount of diffracted light from the parent star to fall on the planet image.

Image displacement in the focal plane during the observation interval smears the image as does any pointing error. Detecting such displacement requires centroiding the central disk of the strong parent star image to a fraction (approximately 1/15) of the diffraction disk diameter. Such a measurement can be done with a quadrant silicon detector, with tracking actuation provided either by small corrections of the telescope axis (body pointing) or small lateral motions of the secondary focus. Roll about the telescope line of sight must be controlled to ~ 0.1 deg.

Reduction of the intensity of the central disk of the planet image is produced by figure error or misalignment aberrations. The energy lost from the planet central disk is proportional to the variance of the amplitude-weighted phase error. Therefore, as apodization increases, the effect of a given wavefront aberration decreases. For a Strehl ratio (= aberrated/unaberrated central intensities) of 0.9, the allowable focus phase error at aperture edge for the APOTS 2 is 1.35 rad (1.94 rad for the APOTS 6).

The increase in the amount of light scattered into the rings of the stellar image from the central disk was calculated for various focus errors using the Hewlett-Packard diffracted light software. The range of assumed phase errors at the aperture edge varied from 0 to π rad. The ratio of the intensities, outer rings/image center, remained nearly constant. Apparently, the energy from the central disk is diffracted only into the inner rings as would be expected for wavefront errors of low spatial frequency.

Table 3 gives the optical parameters and alignment tolerances required for an unapodized telescope for the APOTS 2 and the APOTS 6. Large lateral secondary mirror alignment tolerances imply that image positioning by lateral motion of the secondary mirror (rather than body pointing of the telescope) is acceptable over ranges of tens of μrad.

In summary, we feel that the APOTS pointing and alignment tolerances can be achieved by technology developed for the Space Telescope.

Apodizer

A wide range of apodization techniques has recently been studied by Hewlett-Packard.[2] Only vacuum-deposited metal films on a glass substrate show any promise. Key requirements for apodizer coatings are low light scatter and low wavefront phase distortion in addition to good adherence to the substrate. Rhodium and indium are superior in this regard to other metals. Aluminum, by contrast, has low transmission and high light scatter. Metal film islands must not form in the thin central region of the apodizer film, and the metal film is continuous down to molecular thicknesses. The metal coating introduces phase errors which degrade the APOTS performance by a factor of 2-5 in detection time. The error can, however, be compensated for in large part by refocusing. The substrate material must also be carefully selected and figured with low ripple.

The apodizer should be located near the image of the entrance pupil. The form of the transmission function is not important. Sonine and Gaussian forms were studied since they lend themselves easily to analysis.

Focal Plane

Especially prepared cooled CCD's are promising detectors. They have large spectral and dynamical ranges (0.1-1 μm and 15,000, respectively), large S/N ratio per pixel (450), high photometric precision and accuracy (0.1 and 2%, respectively), high quantum efficiency (0.7 at 6500 Å), low noise read-out (20 pi/pixel), small size (20 μm/pixel), and low power requirements. Since the approximate FOV for each pixel in this application is 0.4 μrad, for a total FOV of ~ 40 μrad (20× standard planet-star angular separation), a 100×100 array would be required, yet 800×800 arrays are already developed. The long detection times of the APOTS 2 will require focal plane cooling to keep the dark current low. The required temperature is 150 K, achieved passively by using a small radiator. Other noise sources (tunneling from substrate and leakage across gate oxidizers) are negligible.

In summary, the APOTS focal plane requirements are well within the present state-of-the-art.

Other Issues

Control of stray light from in-field and out-of-field sources requires a careful optics design and the control of spacecraft contamination. The requirements of the APOTS are similar to that of the Space Telescope whose technology will be used.

On-orbit data processing, data transmission, and spacecraft communication are not critical because the data rate is moderate.

APOTS weight is moderate; therefore, insertion into orbit can be achieved from a low STS orbit by a special orbit boost engine. Engine and propellant choices are listed in Table 4. For efficiency, hydrazine is preferred. After the orbit maneuvers, the spacecraft must be thoroughly outgassed.

V. IRIS: Description and Performance

The IRIS is a two-element shearing infrared interferometer with a baseline (aperture separation) of 13 m, which is rotating about the optical axis (Fig. 6). Its operating wavelength for detection of the standard planet would be 26 μm, which is a compromise between detector availability and S/N. For measuring the planet's temperature, and thereby helping to discriminate against a background star which could be mistaken for a planet, a secondary wavelength of 18 μm would be used.

Table 4 APOTS/IRIS propulsion, $\Delta V = 200$ m/s

Propellant	Specific impulse, s	Propellant required		Exhaust products	Desired thrust (min T/W = 0.01)		Engines available	Remarks
		APOTS	IRIS		APOTS	IRIS		
Nitrogen	60	2840	5920	N_2	>200 lbf	>500 lbf	None	Low technology
Hydrazine (N_2H_4)	220	620	1240	H_2 N_2 NH_3	>150 lbf	>375 lbf	$T = 100$ lbf $T = 300$ lbf	Satisfactory technology
Bipropellant N_2O_4/MMH	320	410	830	CO_2 H_2O N_2O	>140 lbf	>350 lbf	$T = 25$ lbf $T = 100$ lbf $T = 800$ lbf	Satisfactory technology
Oxygen/hydrogen (LO_2/LH_2)	454	290	580	H_2O H_2	>135 lbf	>350 lbf	$T = 15{,}000$ lbf (others investigated)	Satisfactory technology
Electric propulsion	3000	40	83	Hg, Ce, or Ar			$T \simeq 0.030$ lbf (under development)	Long operating time Large solar array Costly

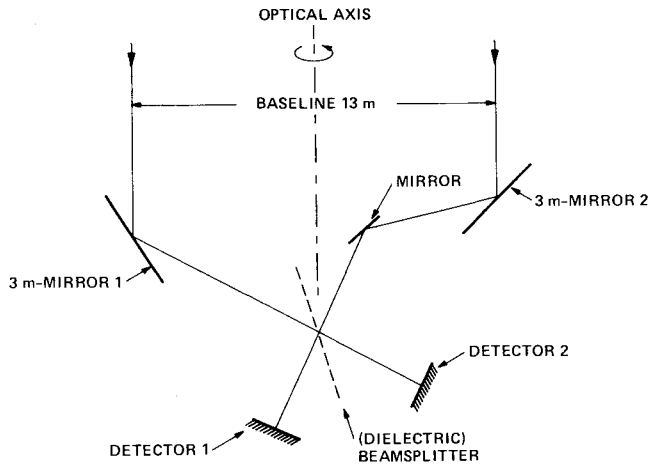

Fig. 6 Spinning interferometer.

In the infrared, detection of the standard planet requires suppression of the Airy disk of the parent star. The IRIS accomplishes suppression by an interferometric null. The two images of a candidate star obtained from the two interferometer arms are superimposed with a phase difference of 180 deg and therefore nulled. The wavefront from the planet is combined with a phase difference depending on its location relative to the star. By rotating the IRIS about the optical axis at the frequency ω, the plant image is moved in a circle about the star, going successively through interferometer nulls and maxima. The planetary signal is thus modulated (ac), while the small residual star signal (=un-nulled photons) is constant (dc). The diffuse sky background (infrared zodiacal light) also gives a dc signal which is in fact much greater than that from un-nulled star photons. Thermal emission by the mirrors must be suppressed below minimum zodiacal by cooling the mirrors to 30 K or less.

The planetary signal contains only even harmonics of ω. From the relative strengths of the harmonics, information about the planet is obtained. We refer to papers by Bracewell and MacPhie for details.[3-6] Since planet detection is identical to the detection of a weak radar echo submerged in noise, we can use radar theory to calculate the probabilities of false alarm and missed-detection in each information channel. These channels, which are the various harmonics, are independent because we cannot predict their relative strengths.

A conceptual design of the IRIS is shown in Fig. 7, and key systems parameters are given in Table 5. Each telescope of the interferometer is afocal and has a parabolic off-axis 3-m beryllium primary and a 10-30-cm-diam secondary mirror in a Gregorian configuration. The secondaries are deployed by separate trusses (graphite/metal structure throughout), which remain folded until final orbit has been achieved. In each telescope, light from the primary mirror enters through a pinhole (serving as field stop) into a light-tight baffle tube, is reflected by the secondary, and enters, by way of relay mirrors, the focal plane dewar. The dewar contains reimaging optics and a second aperture stop. In that dewar, the wavefronts from the two apertures are mixed with a 50% beam splitter and focused on the detectors. The detectors are extrinsic photoconductors, Ge:XX or Si:XX.

If the optical axis of the IRIS does not exactly point to the parent star, a modulated stellar signal is obtained which is indistinguishable from a planet's. For a small pointing error, that signal is nearly all second harmonic. Unless this error can be determined, the 2-ω signal is useless; therefore, it is important that the signal of the planet is strong in higher harmonics, i.e., 4 ω, 6 ω, etc. The choice of a baseline of 13 m satisfies that requirement. This choice also minimizes the standard observation time.** For minimum zodiacal light and reasonable values for detection efficiency and noise, optical transmission, and stray light, the detection time is ~1 h.

Figure 8 shows how the detection time t varies with the key parameters: orbit radius δ, distance d, and angular separation from the parent star θ. Simultaneous use of three signal channels, namely the three lowest harmonics (2 ω, 4 ω, and 6 ω), was assumed. Note that 1) as a fucntion of θ, t has a minimum also at ~1 μrad, but the minimum is mostly second harmonic and therefore susceptible to the IRIS pointing error; nevertheless, given accurate pointing, and with reasonable observation times, the IRIS can detect planets much closer than 2 μrad from the parent star; 2) for $\theta \ll 1$ μrad, $t \propto \theta^{-4}$; and 3) the observation time is a very steep (approximately exponential) function of δ, a behavior caused by the approximately exponential variation of the planetary spectral brightness with temperature which, in turn, is proportional to $\delta^{-1/2}$.

VI. IRIS: Technology Issues

Pointing and Alignment

Achievement of background limited performance depends on the accurate nulling of the star. An incomplete null will produce two errors: a constant component, which would be identified as an increase in background noise; and a time-varying component, which could be mistaken for a planetary signal.

**For a fixed IRIS baseline, 13 m is also near the upper limit allowed by STS payload bay limitations.

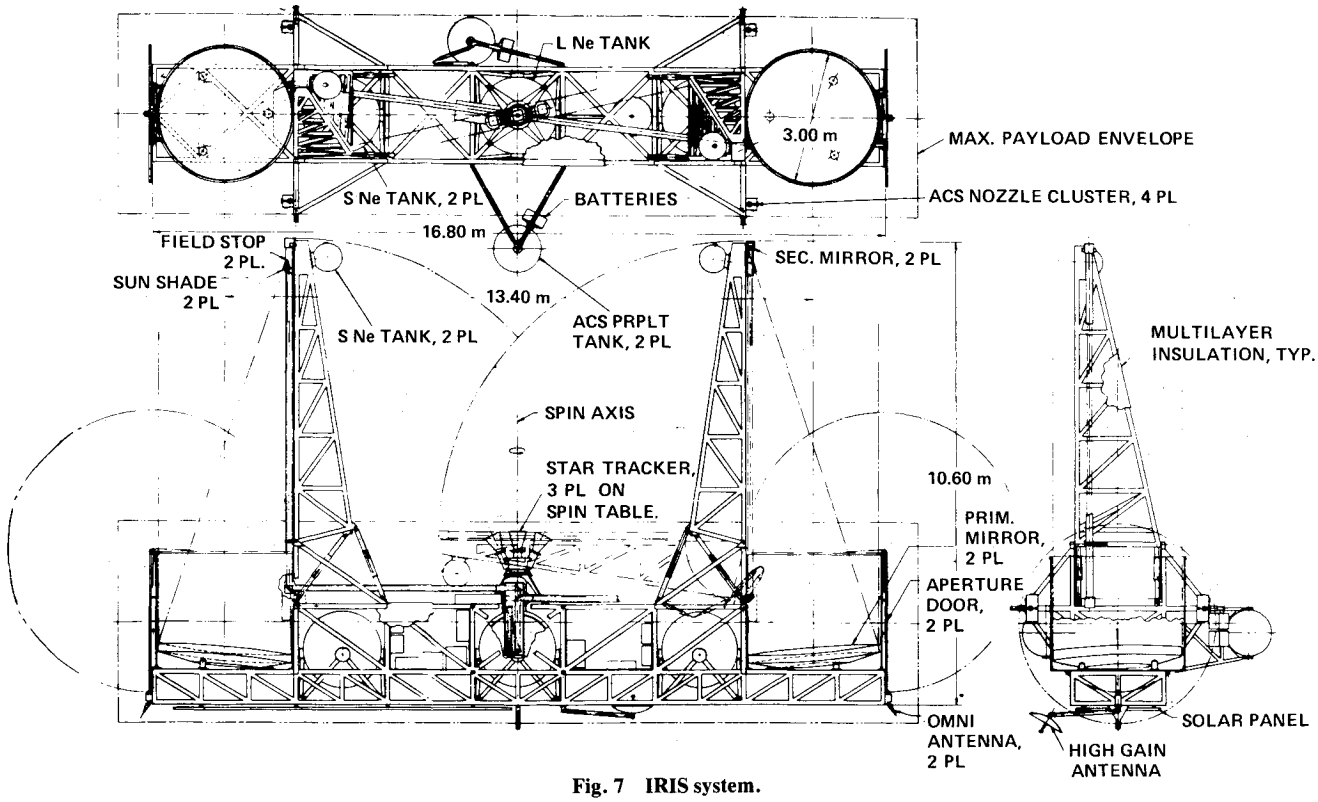

Fig. 7 IRIS system.

Table 5 Spinning infrared interferometers (IRIS's)

Overall dimensions:	Shuttle-bay limits
Total mass:	13,900 kg
Baseline orbit:	550-km circular, 28.5-deg inclination
Delivery and deployment:	Shuttle plus orbit boost engine, no on-orbit assembly
Structure:	Graphite/metal truss
Optics:	Two 3-m-diam, off-axis, parabolic primary f/3 Be mirrors; 2 secondary mirrors; relay optics
Configuration:	Afocal, Gregorian
Interferometer baseline:	13 m
Wavelengths of operation: (standard planet)	26, 18, and 0.55 μm (baseline control)
Detectors:	Extrinsic photoconductors
Cryogenics:	Primary optics—to 30 K via 3100 kg solid neon Focal plane—to 4 K via 310 kg liquid helium

The allowable dc error is taken to be 50% of the zodiacal light. The required interferometer null attenuation factor is $G = 10^{-3}$. This error could be due to amplitude or phase mismatch. In either case, the tolerances are not stringent.

Sources of dc amplitude mismatch include nonuniform transmission of the interferometer legs and beam combiner with unequal transmission and reflection coefficients. An error budget of $G = 5 \times 10^{-4}$ allows a nominally no-loss 50% beam splitter to exhibit any isotropies of up to $\pm 1.5\%$.

It should be noted that the requirements for the telescope figure or alignment are satisfied for $G = 2 \times 10^{-4}$ if the standard deviation of the phase difference between the two aberrated interferometer wavefronts is less than $\lambda/300$ rms. This criterion allows for axial and lateral alignment errors between the primary and secondary mirror foci of 20 and 60 μm, respectively. IRIS telescope alignment requirements are therefore less stringent than those of the Space Telescope, which operates primarily in the visible.

Time-varying (ac) errors are more of a problem. Possible sources of such ac null error are structural distortion, e.g., from gravity gradients and interferometer pointing errors. An error budget is derived from assuming that the spurious harmonic signal may be 50% of the second harmonic signal of the standard planet. Interferometer null factors of 2.5×10^{-6} are required, implying sensing and control of ac optical path differences (OPD's) of $\lambda/2800$ (90 Å at 26 μm).

A technique for achieving such tolerances involves the use of an interferometer null in the visible. Such an approach is planet-insensitive and makes use of the high visible photon flux from the parent star (8×10^9 photon/s/μm). Operating at a nominal wavelength of 0.55 μm, the interferometer would centroid and superimpose the star images. Any OPD change of ± 90 Å would be sensed as an increase from a white-light null to 1% of the maximum signal expected at antinull. The technique appears feasible, though not trivial; it requires that the optics (the beam splitter in particular) be suitable for interferometric operations in the visible as well as in the infrared.

The relative OPD could be corrected by moving the appropriate secondary or relay mirror. The required actuator precision of 50 Å (at low bandwidths) does not stress the state-of-the-art.

The ac signals from the gravity gradient and from small pointing errors are predominantly in the second harmonic (2 ω). Thus, failure of the ac null at 2 ω affects only the IRIS sensitivity for small star-planet separations ($\theta \leq 1.5$ μrad).

Cryogenics

Primary Optics

To keep mirror emission below zodiacal light, all mirrors must be cooled to <30 K. This temperature is not very sensitive to mirror emissivity, assumed to be 0.02. The head load on the primary mirrors is typically 1 w each and is mainly due to conduction through the multilayer insulation and through the fiberglass supports. Solid neon is a plausible choice for cryogen. The amount for a 5-yr mission is 3100 kg (primary and secondary mirrors combined), i.e., about ¼ of the total satellite mass. The cryogen for the primaries is stored in two large tanks in the main structure, and for the secondaries, it is stored in two small tanks at the top of the secondary trusses

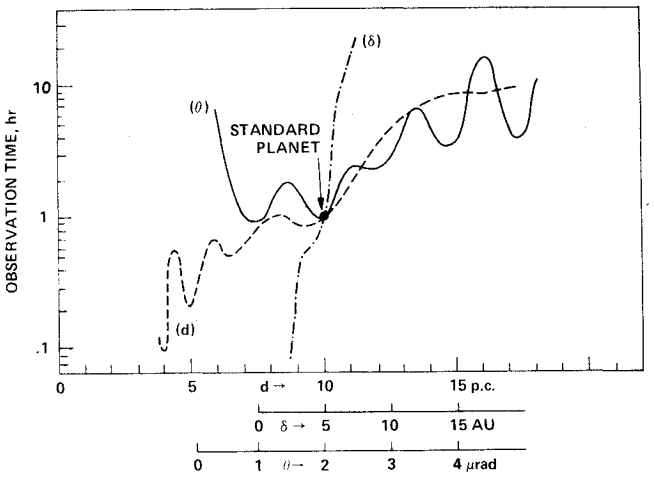

Fig. 8 IRIS performance (three harmonics).

(Fig. 8). Periodic decoupling of the primaries from the cryo-support, for the purpose of boiling off atmospheric condensates, is accomplished by a heat switch of tested design (e.g., a He gas-gap switch).

Solid neon cryogenic systems are well developed, but a 5-yr lifetime system requires careful design to find and eliminate heat leakage paths.

Focal Plane

The focal plane temperature is set by the requirement of low amplifier and detector noise. Ge:Cu requires <4 K, and Si:Sb<8 K. To keep amplifier noise low, large load resistances (10^{13} Ω) are required with MOSFET followers and must be built specifically for this application. A temperature of 4 K could be provided by a liquid helium system, whereas 8 K could be provided by a (more efficient) solid hydrogen system.

Since solid hydrogen cryogenics are as yet inadequately tested and also may involve safety problems, liquid or superfluid helium is preferred. Assuming a single-stage cooling system, 310 kg of liquid helium (or superfluid helium) are sufficient for a 5-yr operation. Superfluid helium systems are not as well developed for liquid helium, but have the advantage of more efficient thermal equalization.

Structural Dynamics

Being a moderately large and flexible rotating structure, the IRIS is subjected to torques and bending stresses (e.g., gyroscopic, gravity-gradient). From a feasibility point, we see no basic technology hurdles. Computer programs can analyze the dynamics of such structures. Such programs integrate the equations of motion which describe the (nonlinear) dynamics of the system.

Graphite/metal space structures can be built sufficiently rigid so that the vehicle bending modes are well outside the attitude pointing controller bandwidth. Therefore, stability considerations due to flexible vehicle controller interactions should not become a significant issue.

Vibration management to control the effects of vibration sources on optical performance will require detailed study. Control moment gyros, reaction wheels, and mass expulsion systems used to maneuver and fine-point the telescope all cause vibrations. Also, vibration from focal plane coolers can produce line-of-sight jitter. Therefore, passive vibration source isolation or active stability augmentation may be required. Further studies must determine any tradeoffs between optical and dynamical control of the IRIS.

IRIS Mirrors

The beryllium mirrors suggested for the IRIS have superior mechanical and thermal properties. High ratios of stiffness/weight and thermal conductivity/thermal expansion (at 30 K), as well as high mirror yield and microcreep strengths, allow for excellent figure stability over long time periods ($\sim\lambda/50$ peak-to-peak in the visible). Previously encountered problems with Be instabilities have been solved with improved material processing. The improvements have made possible the manufacture of highly stable, quality small-scale Be optics at room and cryo temperatures. For the size of mirror considered here, vacuum deposition (under development) may be a preferred manufacturing technique.

Be vapor deposition is done at elevated temperatures. Cooling the mirror to 30 K will cause a figure distortion which can be corrected by one of three methods: 1) figuring the mirror at elevated temperatures so that it will have the proper figure at 30 K; 2) polishing to the correct figure after deposition; this step is made possible by the small grain size and uniformity of the vapor-deposited Be; or 3) applying corrective edge moments to control the figure at 30 K.

Stray Light Control

The secondary and relay mirrors must be enclosed in a baffle tube which is passively cooled to <200 K (cryogen cooling of the entire tube length is difficult to implement). Infrared radiation from this tube will strike the cooled relay optics and reflect nonspecularly onto the detector. Relay mirror superpolishing will reduce this scattered light, but perhaps not below the zodiacal light. Active cooling of the baffle tube section next to the optics may therefore be required.

These additional cooling requirements may substantially impact the design of the cryogenic system of the IRIS and, of course, the ultimate payload capability. A proper study of this impact must await a more detailed systems design, outside the scope of this study.

Some of the radiation scattered from the solar and Earth-illuminated secondary support structure onto the primary mirror will be scattered to the detector. Primary mirror superpolish and baffles on the secondary support structure are required. In summary, a careful study of stray light problems will be necessary.

Table 6 Systems performance

	APOTS 2	APOTS 6	IRIS
Standard observation time t_0	100 h	1 h	1 h
Observation time $t>100$ h	$d\geq 10$ parsec	$d\geq 15$ parsec	$d\geq 30$ parsec
Dependence of t_0 on mirror diameter D	D^{-5}	D^{-9}	D^{-4}
Extreme planet parameter sensitivity	Distance (d^7)	All parameters (e.g., d^{11})	Orbit radius (exponential)
Dominant noise for standard planet observation	Ripple-scattered light of parent star	Diffracted light of parent star	Zodiacal light
Orbit phase effect	Yes	Yes	No
Inherent limitations	Cannot measure planet temperature		Planet position uncertain by 180 deg in azimuth

Table 7 Systems technology

	APOTS 2(6)		IRIS	
	a	*b*	*a*	*b*
Alignment and pointing	1	1	3	2
Apodizer	3	2	...	...
Beam splitter	...	...	3	2
Contamination control	1	1	2	2
Cryogenics	2	1	3	2
Data handling	1	1	1	1
Dynamic control	1	1	3	2
Focal plane	2	1	3	1
Mirror manufacturing	3	2(3)	2	2
Mirror figure control	3	2	1	1
Propulsion	1	1	1	1
Stray light	2	1	2	2
	$c=29(32)$		$c=42$	

Explanation of symbols:
a = systems impact: 1 = important, 2 = substantial impact on performance, 3 = critical, affects feasibility.
b = state-of-the-art: 1 = present/low risk, 2 = advanced/moderate risk, 3 = requires substantial development/high risk.
$c = a \times b$.

Propulsion

Delivery of the IRIS to the operational orbit (550 km circular) is achieved by delivery to standard STS orbit and then boost-up with a special engine. The alternative of Shuttle boost to final orbit, using Orbital Maneuvering Systems Kits, is impractical because it requires shortening the baseline (13 m), thereby reducing the IRIS resolution capability. It is also inefficient.

Contamination considerations affect the propellant and engine choice. Table 4 lists some present options. Cold gas (less contaminating than hydrazine) lacks a developed engine and requires much fuel. An ion engine requires extra-large solar panels, is used only once, and is therefore impractical. If contamination is avoided by allowing a sufficient interval between orbit insertion and deploy, hydrazine is the preferred propellant.

Pointing and retargeting will be accomplished with cold-gas jets, reaction wheels, or gyros.

VII. Comparison of APOTS and IRIS

Performance

Table 6 compares the two sensor systems, giving separate entries for the APOTS 6 and the APOTS 2. The IRIS is superior. For a standard planet, the detection time is less by a factor of ~100 and the range is greater by a factor of 3 (therefore, the detection volume is larger by a factor 27). In addition, the IRIS can detect a nonsolar planet of a given size in closer angular separation from its parent star than the APOTS because its resolution is greater and the planet's infrared brightness does not vary with orbit phase. Finally, a large primary mirror diameter is less critical for the IRIS performance.

The uncertainty in the planet's position measurement by the IRIS can be removed by redesign of the sensor (but at the expense of increased observation time). The extreme sensitivity of the IRIS to planet orbit radius δ is related to the assumed correlation between δ and planet temperature. For some nonsolar planets, the assumption may be invalid.

Technology

Table 7 lists the important technology issues and their relative impact on system feasibility and performance. Some issues require an effort beyond the scope of our study (e.g., dynamical control of the IRIS). By the sensor criticality, defined as $c = a \cdot b$ (a and b are defined in Table 7), the IRIS is technically more demanding than the APOTS. Mass and size of the IRIS are system drivers more so than for the APOTS and are strongly dependent on primary mirror diameter. In theory, the APOTS has the advantage of being a direct imaging system, whereas the IRIS acquires data and reconstructs the parent-star image in a more complicated way. In practice, however, the APOTS data acquisition and evaluation are also complicated because of the complex structure of the focal plane radiation, which has diffracted and scattered light of the parent star and the planet as well as stray and background light.

VIII. Conclusion

It is technically feasible to directly detect planets in other potential solar systems at moderate distances using either the visible or infrared radiation from such planets.

Detection of a Jupiter-like planet around a sun-like star from a distance of 10 parsec (32 light-years) will require an observation time of ~100 h using an apodized visual telescope (APOTS) and 1 h using a spinning infrared interferometer (IRIS). The APOTS has the potential for 1-h observation time, but only with unlikely advances in mirror figure control. The IRIS, on the other hand, requires demonstrations of long-life cryogenics, optical alignment, and dynamical control systems.

Acknowledgments

We are grateful for the support in this work by the Lockheed scientific and technical staff. We also thank L. Hubby (Hewlett-Packard), R. Bracewell (Stanford University), and R. Walker (NASA Ames) for many helpful discussions. This work was supported by NASA Contract No. NAS2-100309, the final report is published under Contractor Report No. NASA-CR-152253.

References

[1] Oliver, B.M., "Planetary Detection by Direct Optical Imaging," presented at 2nd NASA Workshop on Planetary Detection, Ames Research Center, Moffett Field, Calif., May 1976.

[2] Hewlett-Packard, Interim Report, NASA Contract NAS2-9786, 1978.

[3] MacPhie, R.H. and Bracewell, R.N., "Investigation of Planetary Search Technique by Infrared Interferometry," Final Report, NASA Contract NCA2-OR745-716, 1978.

[4] Bracewell, R.N., "Detecting Nonsolar Planets by Spinning Infrared Interferometer," *Nature*, Vol. 274, Aug. 24, 1978, pp. 780-781.

[5] Bracewell, R.N. and MacPhie, R.H., "Searching for Nonsolar Planets," *Icarus*, Vol. 38, Jan. 1979, pp. 136-147.

[6] MacPhie, R.H., and Bracewell, R.N., "An Orbiting Infrared Interferometer to Search for Nonsolar Planets," *SPIE Conference Proceedings*, Tucson, Ariz., Jan. 29-Feb. 1, 1979, pp. 271-278.